



SNS COLLEGE OF TECHNOLOGY

(An Autonomous Institution)

Approved by AICTE, New Delhi, Affiliated to Anna University, Chennai

Accredited by NAAC-UGC with 'A++' Grade (Cycle III) &

Accredited by NBA (B.E - CSE, EEE, ECE, Mech & B.Tech. IT)

COIMBATORE-641 035, TAMIL NADU



DEPARTMENT OF AEROSPACE ENGINEERING

Faculty Name : **Dr.A.Arun Negemiya,** Academic Year : **2024-2025 (Even)**
ASP/ Aero
Year & Branch : **III AEROSPACE** Semester : **VI**
Course : **19ASB304 - Computational Fluid Dynamics for Aerospace Application**

UNIT V – FLOW FIELD ANALYSIS AND TURBULENCE MODELS

Low Reynolds Number Models

In the previous section, we discussed all the functions that are used to reduce the number of cells. However, we must be aware that this is an approximation which, if the flow near the boundary is important, can be rather crude. In many internal flows – where all boundaries are either walls, symmetry planes, inlets, or outlets – the boundary layer may not be that important, as the flow field is often pressure-determined. For external flows (for example flow around cars, ships, airplanes, etc.), however, the flow conditions in the boundaries are almost invariably important. When we are predicting heat transfer it is in general a good idea to use wall functions because the heat transfer at the walls is very important for the temperature field in the whole domain.

When we choose not to use wall functions, we thus insert sufficiently many grid lines near solid boundaries so that the boundary layer can be adequately resolved. However, when the wall is approached the viscous effects become more important and for $y^+ < 5$ the flow is viscous dominating, i.e. the viscous diffusion is much larger than the turbulent one (see Fig. 4.1). Thus, the turbulence models presented so far may not be correct since fully turbulent conditions have been assumed; this type of models are often referred to as high-Re number models. In this section, we will discuss modifications of high-Re number models so that they can be used down to the wall. These modified models are termed low Reynolds number models. Please note that “high Reynolds number” and “low Reynolds number” do not refer to the global Reynolds number (for example Re_L , Re_x , Re_δ , etc.) but here we are talking about the local turbulent Reynolds number $Re_\ell = U\ell/\nu$ formed by a turbulent fluctuation and turbulent length scale. This Reynolds number varies throughout the computational domain and is proportional to the ratio

of the turbulent and physical viscosity ν_t/ν , i.e. $Re_\ell \propto \nu_t/\nu$. This ratio is 100 or more prominent in fully turbulent flow and goes to zero when a wall is approached.

We start by studying how various quantities behave close to the wall when $y \rightarrow 0$. Taylor expansion of the fluctuating velocities u_i (also valid for the mean velocities \bar{U}_i) gives

$$\begin{aligned} u &= a_0 + a_1 y + a_2 y^2 \dots \\ v &= b_0 + b_1 y + b_2 y^2 \dots \\ w &= c_0 + c_1 y + c_2 y^2 \dots \end{aligned} \tag{4.1}$$

where $a_0 \dots c_2$ are functions of space and time. At the wall, we have no slip, i.e. $u = v = w = 0$ which gives $a_0 = b_0 = c_0$. Furthermore, at the wall $\partial u/\partial x = \partial w/\partial z = 0$, and the continuity equation gives $\partial v/\partial y = 0$ so that

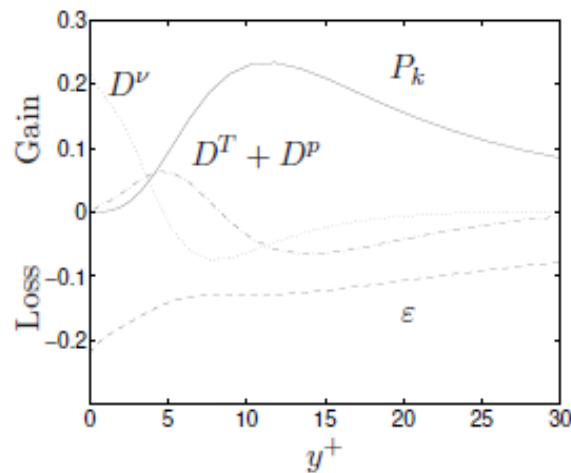


Figure 4.1: Flow between two parallel plates. Direct numerical simulations [24]. $Re = U_C \delta/\nu = 7890$. $u_*/U_C = 0.050$. Energy balance in k equation. Production P_k , dissipation ϵ , turbulent diffusion (by velocity triple correlations and pressure) $D^T + D^P$, and viscous diffusion D^ν . All terms have been scaled with u_*^4/ν .

$b_1 = 0$. Equation 4.1 can now be written

$$\begin{aligned} u &= a_1 y + a_2 y^2 \dots \\ v &= b_2 y^2 \dots \\ w &= c_1 y + c_2 y^2 \dots \end{aligned} \tag{4.2}$$

From Eq. 4.2 we immediately get

$$\begin{aligned} \overline{u^2} &= \overline{a_1^2 y^2} \dots = \mathcal{O}(y^2) \\ \overline{v^2} &= \overline{b_2^2 y^4} \dots = \mathcal{O}(y^4) \\ \overline{w^2} &= \overline{c_1^2 y^2} \dots = \mathcal{O}(y^2) \\ \overline{uv} &= \overline{a_1 b_2 y^3} \dots = \mathcal{O}(y^3) \\ k &= \overline{(a_1^2 + c_1^2) y^2} \dots = \mathcal{O}(y^2) \\ \partial \bar{U} / \partial y &= \overline{a_1} \dots = \mathcal{O}(y^0) \end{aligned} \tag{4.3}$$

In Fig. 4.2 DNS-data for the fully developed flow in a channel is presented.

4.1 Low-Re $k - \varepsilon$ Models

There exist a number of Low-Re number $k - \varepsilon$ models [35, 7, 10, 1, 30]. When deriving low-Re models it is common to study the behavior of the terms when $y \rightarrow 0$ in the exact equations and require that the corresponding terms in the modelled equations behave in the same way. Let us study

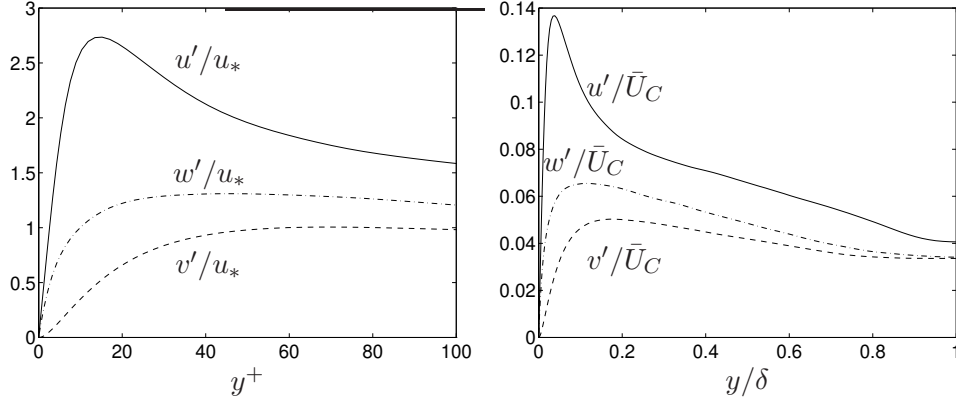


Figure 4.2: Flow between two parallel plates. Direct numerical simulations [24]. $Re = U_C \delta / \nu = 7890$. $u_* / U_C = 0.050$. Fluctuating velocity components $u'_i = \sqrt{u_i'^2}$.

the exact k equation near the wall (see Eq. 2.24).

$$\begin{aligned} \frac{\partial \rho \bar{U} k}{\partial x} + \frac{\partial \rho \bar{V} k}{\partial y} &= \underbrace{-\rho \bar{u} v \frac{\partial \bar{U}}{\partial y}}_{\mathcal{O}(y^3)} - \frac{\partial \bar{p} v}{\partial y} - \underbrace{\frac{\partial}{\partial y} \left(\frac{1}{2} \rho \bar{v} u_i u_i \right)}_{\mathcal{O}(y^3)} \\ &+ \mu \frac{\partial^2 k}{\partial y^2} - \underbrace{\mu \bar{u}_{i,j} \bar{u}_{i,j}}_{\mathcal{O}(y^0)} \end{aligned} \quad (4.4)$$

The pressure diffusion $\partial \bar{p} v / \partial y$ term is usually neglected, partly because it is not measurable, and partly because close to the wall it is not important, see Fig. 4.3 (see also [31]). The modelled equation reads

$$\begin{aligned} \frac{\partial \rho \bar{U} k}{\partial x} + \frac{\partial \rho \bar{V} k}{\partial y} &= \underbrace{\mu_t \left(\frac{\partial \bar{U}}{\partial y} \right)^2}_{\mathcal{O}(y^4)} + \underbrace{\frac{\partial}{\partial y} \left(\frac{\mu_t}{\sigma_k} \frac{\partial k}{\partial y} \right)}_{\mathcal{O}(y^4)} \\ &+ \mu \frac{\partial^2 k}{\partial y^2} - \underbrace{\rho \varepsilon}_{\mathcal{O}(y^0)} \end{aligned} \quad (4.5)$$

When arriving at that the production term is $\mathcal{O}(y^4)$ we have used

$$\nu_t = c_\mu \rho \frac{k^2}{\varepsilon} = \frac{\mathcal{O}(y^4)}{\mathcal{O}(y^0)} = \mathcal{O}(y^4) \quad (4.6)$$

Comparing Eqs. 4.4 and 4.5 we find that the dissipation term in the modelled equation behaves in the same way as in the exact equation when

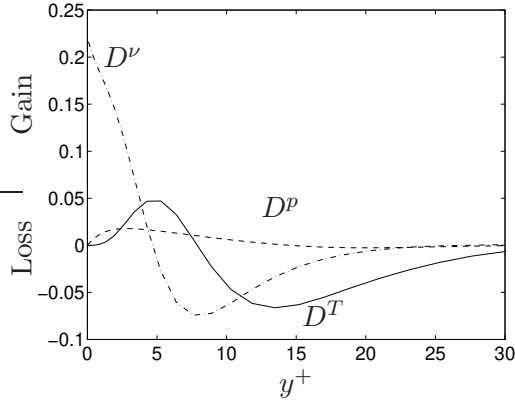


Figure 4.3: Flow between two parallel plates. Direct numerical simulations [24]. $Re = U_C \delta / \nu = 7890$. $u_* / U_C = 0.050$. Energy balance in k equation. Turbulent diffusion by velocity triple correlations D^T , Turbulent diffusion by pressure D^p , and viscous diffusion D^ν . All terms have been scaled with u_*^4 / ν .

$y \rightarrow 0$. However, both the modelled production and the diffusion term are of $\mathcal{O}(y^4)$ whereas the exact terms are of $\mathcal{O}(y^3)$. This inconsistency of the modelled terms can be removed by replacing the c_μ constant by $c_\mu f_\mu$ where f_μ is a damping function f_μ so that $f_\mu = \mathcal{O}(y^{-1})$ when $y \rightarrow 0$ and $f_\mu \rightarrow 1$ when $y^+ \geq 50$. Please note that the term “damping term” in this case is not correct since f_μ actually is augmenting μ_t when $y \rightarrow 0$ rather than damping. However, it is common to call all low-Re number functions for “damping functions”.

Instead of introducing a damping function f_μ , we can choose to solve for a modified dissipation which is denoted $\tilde{\varepsilon}$, see Ref. [28] and Section 4.2.

It is possible to proceed in the same way when deriving damping functions for the ε equation [42]. An alternative way is to study the modelled ε equation near the wall and keep only the terms which do not tend to zero. From Eq. 3.3 we get

$$\begin{aligned}
 \underbrace{\frac{\partial \rho \bar{U} \varepsilon}{\partial x}}_{\mathcal{O}(y^1)} + \underbrace{\frac{\partial \rho \bar{V} \varepsilon}{\partial y}}_{\mathcal{O}(y^1)} &= \underbrace{c_{\varepsilon 1} \frac{\varepsilon}{k} P_k}_{\mathcal{O}(y^1)} + \underbrace{\frac{\partial}{\partial y} \left(\frac{\mu_t}{\sigma_\varepsilon} \frac{\partial \varepsilon}{\partial y} \right)}_{\mathcal{O}(y^2)} \\
 &+ \underbrace{\mu \frac{\partial^2 \varepsilon}{\partial y^2}}_{\mathcal{O}(y^0)} - \underbrace{c_{\varepsilon 2} \rho \frac{\varepsilon^2}{k}}_{\mathcal{O}(y^{-2})}
 \end{aligned} \tag{4.7}$$

where it has been assumed that the production term P_k has been suitable modified so that $P_k = \mathcal{O}(y^3)$. We find that the only term which do not vanish at the wall are the viscous diffusion term and the dissipation term

so that close to the wall the dissipation equation reads

$$0 = \mu \frac{\partial^2 \varepsilon}{\partial y^2} - c_{\varepsilon 2} \rho \frac{\varepsilon^2}{k}. \quad (4.8)$$

The equation needs to be modified since the diffusion term cannot balance the destruction term when $y \rightarrow 0$.

4.2 The Launder-Sharma Low-Re $k - \varepsilon$ Models

There are at least a dozen different low Re $k - \varepsilon$ models presented in the literature. Most of them can be cast in the form [35] (in boundary-layer form, for convenience)

$$\frac{\partial \rho \bar{U} k}{\partial x} + \frac{\partial \rho \bar{V} k}{\partial y} = \frac{\partial}{\partial y} \left[\left(\mu + \frac{\mu_t}{\sigma_k} \right) \frac{\partial k}{\partial y} \right] + \mu_t \left(\frac{\partial \bar{U}}{\partial y} \right)^2 - \rho \varepsilon \quad (4.9)$$

$$\begin{aligned} \frac{\partial \rho \bar{U} \tilde{\varepsilon}}{\partial x} + \frac{\partial \rho \bar{V} \tilde{\varepsilon}}{\partial y} = & \frac{\partial}{\partial y} \left[\left(\mu + \frac{\mu_t}{\sigma_\varepsilon} \right) \frac{\partial \tilde{\varepsilon}}{\partial y} \right] + c_{1\varepsilon} f_1 \frac{\tilde{\varepsilon}}{k} \mu_t \left(\frac{\partial \bar{U}}{\partial y} \right)^2 \\ & - c_{\varepsilon 2} f_2 \rho \frac{\tilde{\varepsilon}^2}{k} + E \end{aligned} \quad (4.10)$$

$$\mu_t = c_\mu f_\mu \rho \frac{k^2}{\tilde{\varepsilon}} \quad (4.11)$$

$$\varepsilon = \tilde{\varepsilon} + D \quad (4.12)$$

Different models use different damping functions (f_μ , f_1 and f_2) and different extra terms (D and E). Many models solve for $\tilde{\varepsilon}$ rather than for ε where D is equal to the wall value of ε which gives an easy boundary condition $\tilde{\varepsilon} = 0$ (see Sub-section 4.3). Other models which solve for ε use no extra source in the k equation, i.e. $D = 0$.

Below we give some details for one of the most popular low-Re $k - \varepsilon$ models, the Launder-Sharma model [28] which is based on the model of Jones & Launder [23]. The model is given by Eqs. 4.9, 4.10, 4.11 and 4.12 **Launder-Sharma**

where

$$\begin{aligned}
f_\mu &= \exp\left(\frac{-3.4}{(1 + R_T/50)^2}\right) \\
f_1 &= 1 \\
f_2 &= 1 - 0.3 \exp(-R_T^2) \\
D &= 2\mu \left(\frac{\partial\sqrt{k}}{\partial y}\right)^2 \\
E &= 2\mu \frac{\mu_t}{\rho} \left(\frac{\partial^2\bar{U}}{\partial y^2}\right)^2 \\
R_T &= \frac{k^2}{\nu\tilde{\varepsilon}}
\end{aligned} \tag{4.13}$$

The term E was added to match the experimental peak in k around $y^+ \simeq 20$ [23]. The f_2 term is introduced to mimic the final stage of decay of turbulence behind a turbulence generating grid when the exponent in $k \propto x^{-m}$ changes from $m = 1.25$ to $m = 2.5$.

4.3 Boundary Condition for ε and $\tilde{\varepsilon}$

In many low-Re $k - \varepsilon$ models $\tilde{\varepsilon}$ is the dependent variable rather than ε . The main reason is that the boundary condition for ε is rather complicated. The largest term in the k equation (see Eq. 4.4) close to the wall, are the dissipation term and the viscous diffusion term which both are of $\mathcal{O}(y^0)$ so that

$$0 = \mu \frac{\partial^2 k}{\partial y^2} - \rho\varepsilon. \tag{4.14}$$

From this equation we get immediately a boundary condition for ε as

$$\varepsilon_{wall} = \nu \frac{\partial^2 k}{\partial y^2}. \tag{4.15}$$

From Eq. 4.14 we can derive alternative boundary conditions. The exact form of the dissipation term close to the wall reads (see Eq. 2.24)

$$\varepsilon = \nu \left\{ \left(\frac{\partial u}{\partial y}\right)^2 + \left(\frac{\partial w}{\partial y}\right)^2 \right\} \tag{4.16}$$

where $\partial/\partial y \gg \partial/\partial x \simeq \partial/\partial z$ and $\partial u/\partial y \simeq \partial w/\partial y \gg \partial v/\partial y$ have been assumed. Using Taylor expansion in Eq. 4.1 gives

$$\varepsilon = \nu \left(\overline{a_1^2} + \overline{c_1^2} \right) + \dots \tag{4.17}$$

In the same way we get an expression for the turbulent kinetic energy

$$k = \frac{1}{2} (\overline{a_1^2} + \overline{c_1^2}) y^2 \dots \quad (4.18)$$

so that

$$\left(\frac{\partial \sqrt{k}}{\partial y} \right)^2 = \frac{1}{2} (\overline{a_1^2} + \overline{c_1^2}) \dots \quad (4.19)$$

Comparing Eqs. 4.17 and 4.19 we find

$$\varepsilon_{wall} = 2\nu \left(\frac{\partial \sqrt{k}}{\partial y} \right)^2. \quad (4.20)$$

In the Sharma-Launder model this is exactly the expression for D in Eqs. 4.12 and 4.13, which means that the boundary condition for $\tilde{\varepsilon}$ is zero, i.e. $\tilde{\varepsilon} = 0$.

In the model of Chien [8], the following boundary condition is used

$$\varepsilon_{wall} = 2\nu \frac{k}{y^2} \quad (4.21)$$

This is obtained by assuming $a_1 = c_1$ in Eqs. 4.17 and 4.18 so that

$$\begin{aligned} \varepsilon &= 2\nu \overline{a_1^2} \\ k &= \overline{a_1^2} y^2 \end{aligned} \quad (4.22)$$

which gives Eq. 4.21.

4.4 The Two-Layer $k - \varepsilon$ Model

Near the walls the one-equation model by Wolfshtein [51], modified by Chen and Patel [7], is used. In this model the standard k equation is solved; the diffusion term in the k -equation is modelled using the eddy viscosity assumption. The turbulent length scales are prescribed as [16, 11]

$$\ell_\mu = c_\ell n [1 - \exp(-R_n/A_\mu)], \quad \ell_\varepsilon = c_\ell n [1 - \exp(-R_n/A_\varepsilon)]$$

(n is the normal distance from the wall) so that the dissipation term in the k -equation and the turbulent viscosity are obtained as:

$$\varepsilon = \frac{k^{3/2}}{\ell_\varepsilon}, \quad \mu_t = c_\mu \rho \sqrt{k} \ell_\mu \quad (4.23)$$

The Reynolds number R_n and the constants are defined as

$$R_n = \frac{\sqrt{k}n}{\nu}, \quad c_\mu = 0.09, \quad c_\ell = \kappa c_\mu^{-3/4}, \quad A_\mu = 70, \quad A_\varepsilon = 2c_\ell$$

The one-equation model is used near the walls (for $R_n \leq 250$), and the standard high-Re $k - \varepsilon$ in the remaining part of the flow. The matching line could either be chosen along a pre-selected grid line, or it could be defined as the cell where the damping function

$$1 - \exp(-R_n/A_\mu)$$

takes, e.g., the value 0.95. The matching of the one-equation model and the $k - \varepsilon$ model does not pose any problems but gives a smooth distribution of μ_t and ε across the matching line.

4.5 The low-Re $k - \omega$ Model

A model which is being used more and more is the $k - \omega$ model of Wilcox [48]. The standard $k - \omega$ model can actually be used all the way to the wall without any modifications [48, 32, 37]. One problem is the boundary condition for ω at walls since (see Eq. 3.26)

$$\omega = \frac{\varepsilon}{\beta^* k} = \mathcal{O}(y^{-2}) \quad (4.24)$$

tends to infinity. In Sub-section 4.3 we derived boundary conditions for ε by studying the k equation close to the wall. In the same way we can here use the ω equation (Eq. 3.26) close to the wall to derive a boundary condition for ω . The largest terms in Eq. 3.26 are the viscous diffusion term and the destruction term, i.e.

$$0 = \mu \frac{\partial^2 \omega}{\partial y^2} - c_{\omega 2} \rho \omega^2. \quad (4.25)$$

The solution to this equation is

$$\omega = \frac{6\nu}{c_{\omega 2} y^2} \quad (4.26)$$

The ω equation is normally not solved close to the wall but for $y^+ < 2.5$, ω is computed from Eq. 4.26, and thus no boundary condition is actually needed. This works well in finite volume methods but when finite element methods are used ω is needed *at* the wall. A slightly different approach must then be used [17].

Wilcox has also proposed a $k - \omega$ model [50] which is modified for viscous effects, i.e. a true low-Re model with damping function. He demonstrates that this model can predict transition and claims that it can be used for taking the effect of surface roughness into account which later has been confirmed [36]. A modification of this model has been proposed in [39].

4.5.1 The low-Re $k - \omega$ Model of Peng et al.

The $k - \omega$ model of Peng *et al.* reads [39]

$$\begin{aligned}
\frac{\partial k}{\partial t} + \frac{\partial}{\partial x_j}(\bar{U}_j k) &= \frac{\partial}{\partial x_j} \left[\left(\nu + \frac{\nu_t}{\sigma_k} \right) \frac{\partial k}{\partial x_j} \right] + P_k - c_k f_k \omega k \\
\frac{\partial \omega}{\partial t} + \frac{\partial}{\partial x_j}(\bar{U}_j \omega) &= \frac{\partial}{\partial x_j} \left[\left(\nu + \frac{\nu_t}{\sigma_\omega} \right) \frac{\partial \omega}{\partial x_j} \right] + \frac{\omega}{k} (c_{\omega 1} f_\omega P_k - c_{\omega 2} k \omega) + c_\omega \frac{\nu_t}{k} \left(\frac{\partial k}{\partial x_j} \frac{\partial \omega}{\partial x_j} \right) \\
\nu_t &= f_\mu \frac{k}{\omega} \\
f_k &= 1 - 0.722 \exp \left[- \left(\frac{R_t}{10} \right)^4 \right] \\
f_\mu &= 0.025 + \left\{ 1 - \exp \left[- \left(\frac{R_t}{10} \right)^{3/4} \right] \right\} \\
&\quad \left\{ 0.975 + \frac{0.001}{R_t} \exp \left[- \left(\frac{R_t}{200} \right)^2 \right] \right\} \\
f_\omega &= 1 + 4.3 \exp \left[- \left(\frac{R_t}{1.5} \right)^{1/2} \right], \quad f_\omega = 1 + 4.3 \exp \left[- \left(\frac{R_t}{1.5} \right)^{1/2} \right] \\
c_k &= 0.09, \quad c_{\omega 1} = 0.42, \quad c_{\omega 2} = 0.075 \\
c_\omega &= 0.75, \quad \sigma_k = 0.8, \quad \sigma_\omega = 1.35
\end{aligned} \tag{4.27}$$

4.5.2 The low-Re $k - \omega$ Model of Bredberg et al.

A new $k - \omega$ model was recently proposed by Bredberg *et al.* [5] which reads

$$\begin{aligned}
\frac{\partial k}{\partial t} + \frac{\partial}{\partial x_j}(\bar{U}_j k) &= P_k - C_k k \omega + \frac{\partial}{\partial x_j} \left[\left(\nu + \frac{\nu_t}{\sigma_k} \right) \frac{\partial k}{\partial x_j} \right] \\
\frac{\partial \omega}{\partial t} + \frac{\partial}{\partial x_j}(\bar{U}_j \omega) &= C_{\omega 1} \frac{\omega}{k} P_k - C_{\omega 2} \omega^2 + \\
&\quad C_\omega \left(\frac{\nu}{k} + \frac{\nu_t}{k} \right) \frac{\partial k}{\partial x_j} \frac{\partial \omega}{\partial x_j} + \frac{\partial}{\partial x_j} \left[\left(\nu + \frac{\nu_t}{\sigma_\omega} \right) \frac{\partial \omega}{\partial x_j} \right]
\end{aligned} \tag{4.28}$$

The turbulent viscosity is given by

$$\begin{aligned}
\nu_t &= C_\mu f_\mu \frac{k}{\omega} \\
f_\mu &= 0.09 + \left(0.91 + \frac{1}{R_t^3} \right) \left[1 - \exp \left\{ - \left(\frac{R_t}{25} \right)^{2.75} \right\} \right]
\end{aligned} \tag{4.29}$$

with the turbulent Reynolds number defined as $R_t = k/(\omega\nu)$. The constants in the model are given as

$$\begin{aligned} C_k &= 0.09, & C_\mu &= 1, & C_\omega &= 1.1, & C_{\omega 1} &= 0.49, \\ C_{\omega 2} &= 0.072, & \sigma_k &= 1, & \sigma_\omega &= 1.8 \end{aligned} \tag{4.30}$$